Testing of a Steel Deck Bridge

G. W. ZUURBIER, Bethlehem Steel Corporation

•THIS paper concerns the testing of an experimental bridge built by Bethlehem Steel Corporation at its Sparrows Point, Md., plant in 1964. The bridge was built to explore the use of prefabricated all-steel modular units for the construction of highway bridges in the span range of 20 to 100 ft.

A cross section of an individual unit is shown in Figure 1. A continuous corrugated stiffener plate, $^{3}/_{16}$ in. thick, is attached to a $^{3}/_{16}$-in. flat deck plate by means of a burn-through submerged-arc weld, to form a deck assembly 8 ft wide and 56 ft long (Fig. 2). Two T-sections are welded to the deck assembly, to form the webs and bottom flanges (Fig. 3).

Transverse bars are inserted through slots in the webs, at 4-ft centers, for floor beams. The bars are welded to the webs and also to the lower surface of the corrugations (Fig. 4). The two holes at each end of the bars accommodate a bolted splice which is designed to transmit vertical shear between adjacent units in the assembled structure.

Angle diaphragms are located at each end and at the center of the unit. With other incidental details, this forms the complete unit (Fig. 5).

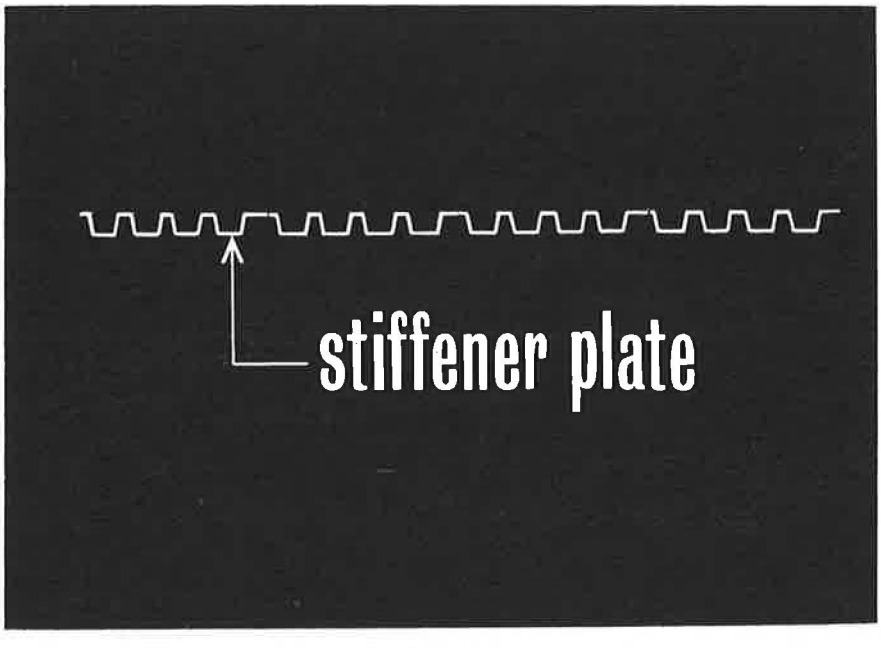

Figure 1.

Paper sponsored by Committee on Steel Superstructures and presented at the 47th Annual Meeting.

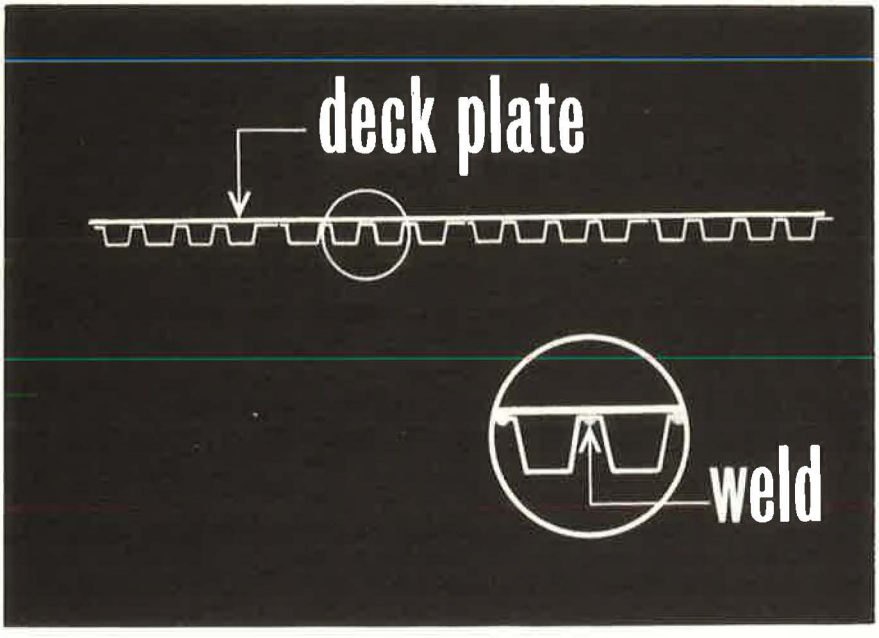

Figure 2.

The unit is completely painted, and given a coal-tar epoxy and sand membrane coating on the deck surface prior to leaving the shop (Fig. 6).

The static behavior of a single unit was studied by placing two of these units in a test rig in the shop (Fig. 7), using one of the units as a frame for loading against the other. The lower unit in Figure 7 is being tested.

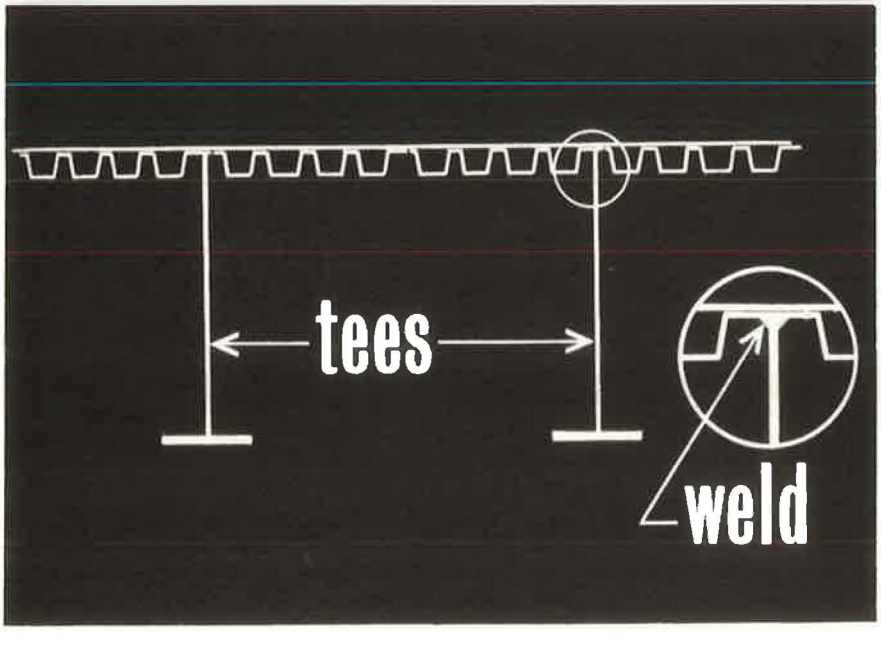

Figure 3.

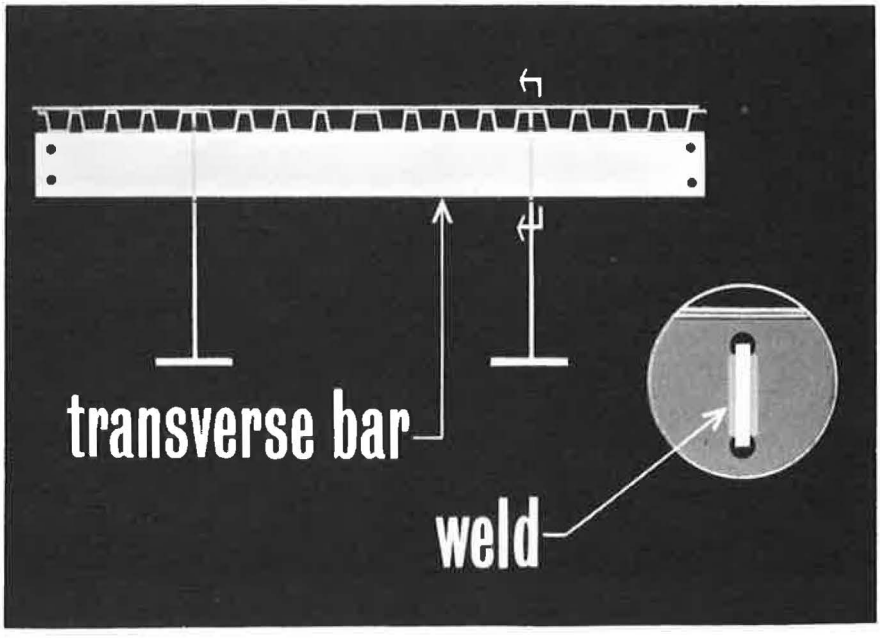

Figure 4.

Electrical resistance strain gages were applied, and output from these gages was carried by cables to a terminal board housed in a nearby test trailer (Figs. 8 and 9). Loads were applied with hydraulic jacks (Fig.10).

The output from 96 gages was recorded in approximately three minutes for each test loading, using an automatic strain gage recorder (Fig. 11), which presented the data visually on graph paper.

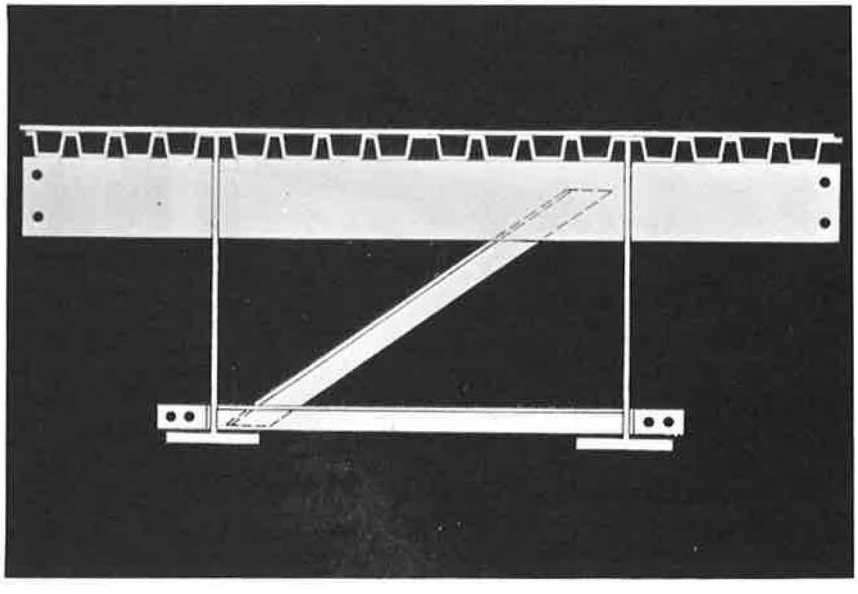

Figure 5.

Figure 6.

Data were also recorded in punched card form on IBM card punch equipment. In Figure 12, the operator is placing input data on a card, before proceeding with the automatic recording of data for a given test sequence. The primary reduction of data was made later from these cards, using the graphical recording mainly for backup and checking purposes.

One calculation confirmed by this test was that the entire width of the deck-assembly participated uniformly in resisting overall bending in the unit, as shown by stress

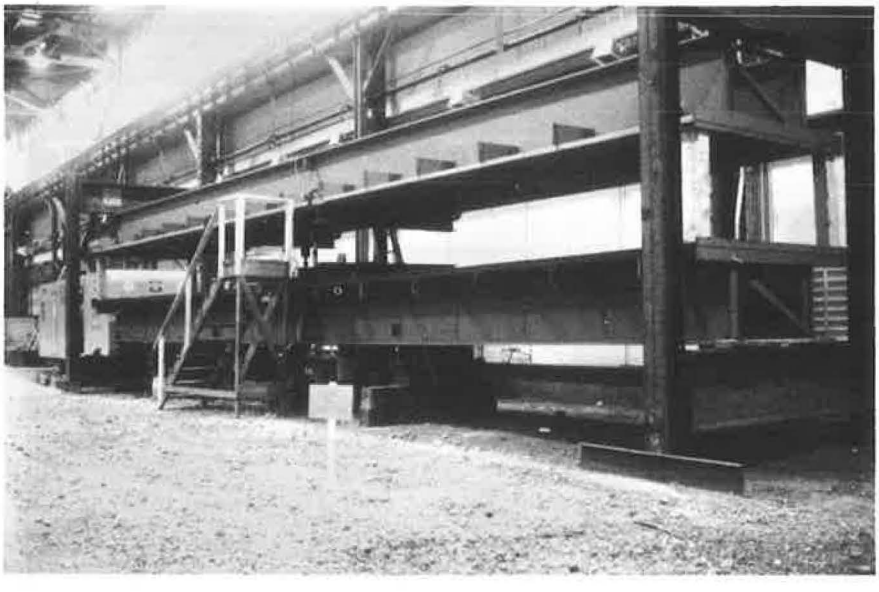

Figure 7.

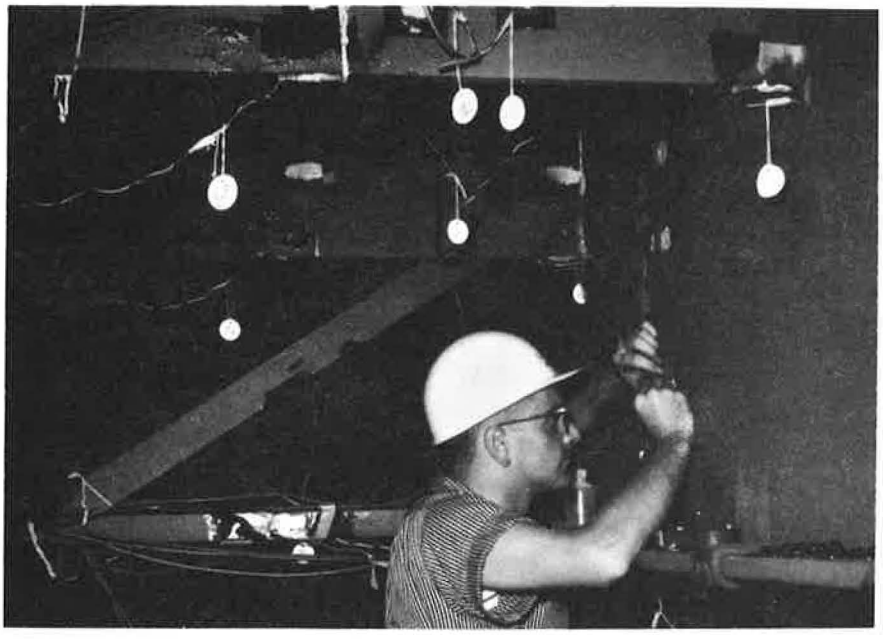

Figure 8.

readings (Fig. 13) at various stages of loading. The horizontal dashed lines represent predicted stress levels. The test also indicated that the experimental location of the neutral axis was very close to the calculated location as shown by the general convergence of stress lines at the approximate predicted location (Fig. 14). The comforting

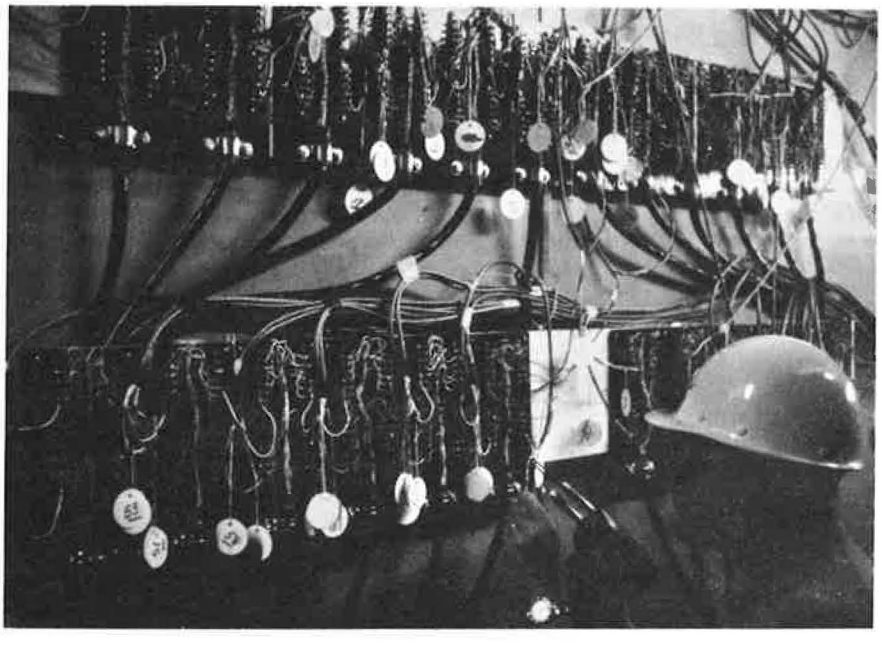

Figure 9.

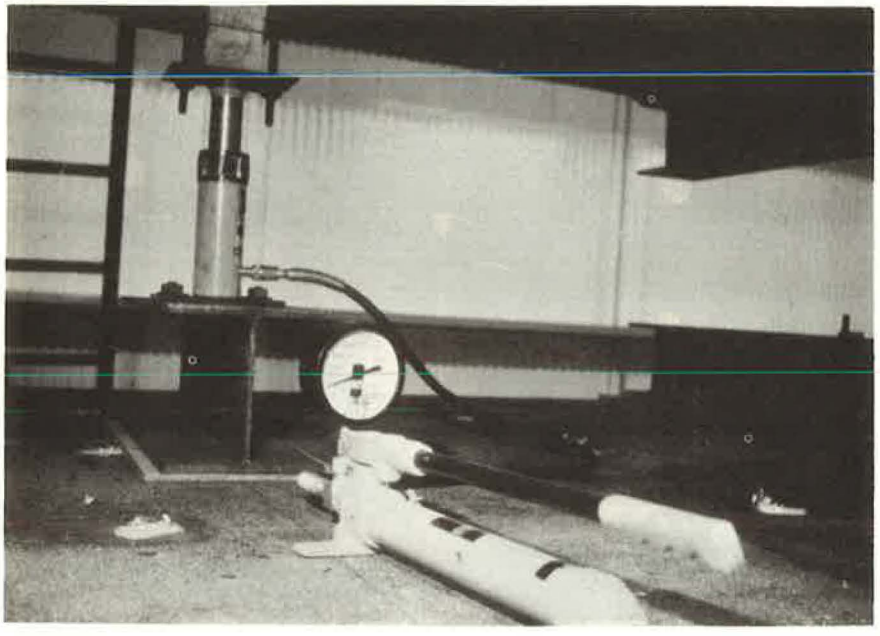

Figure 10.

significance of this result is, of course, that conventional rules of behavior apply to this type of structure, and that stresses throughout the depth of the unit, due to overall bending, can be accurately predicted by the familiar equation of "stress equals Mc/I." This test also proof-loaded the unit.

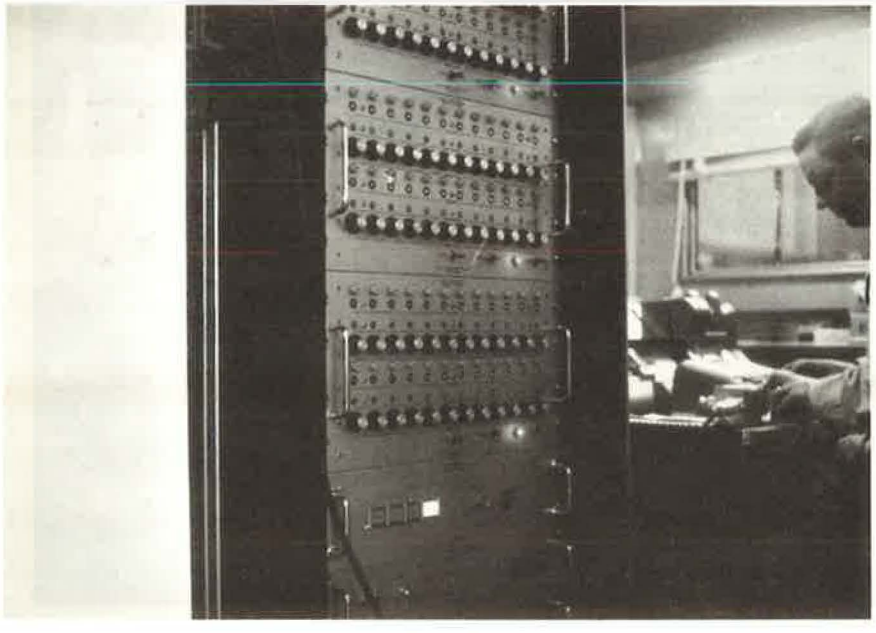

Figure 11.

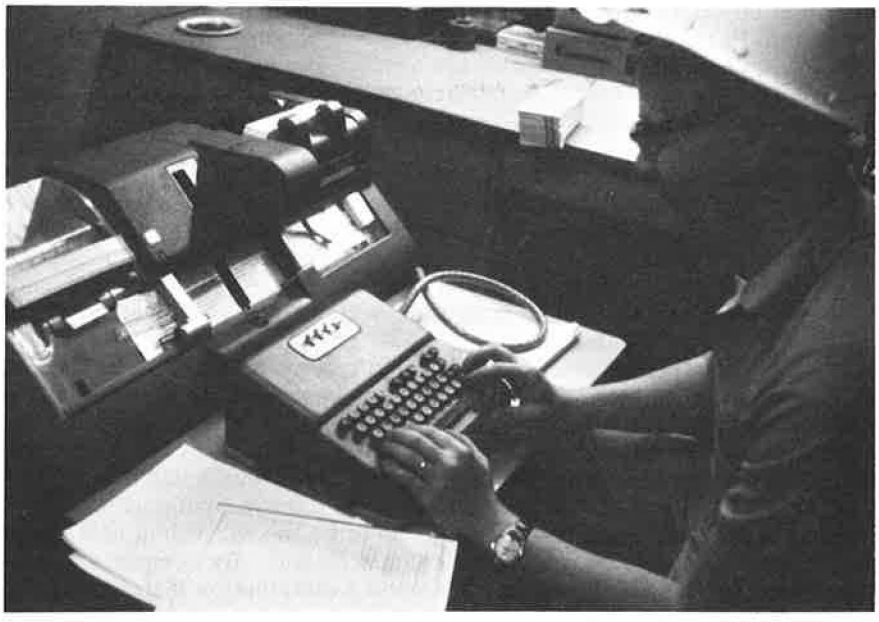

Figure 12.

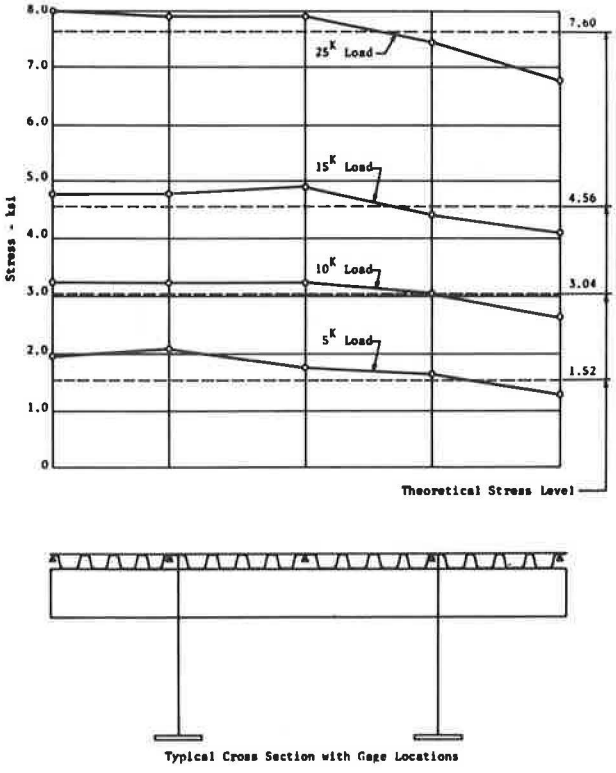

Figure 13. Stress distribution in compression flange—shop test.

The next test objective was to determine the distribution of wheel loads to the webs and to the bottom flanges of multiple units in overall bending, by test-loading in the field with various vehicles. Figure 15 shows the off-highway earth mover that was used as the design vehicle for this structure. It produces overall bending moments about 15 percent greater than an AASHO HS-20 truck.

Figure 16 shows the standard HS-20 truck. Both vehicles were used in obtaining wheel-load distribution factors. This distribution factor is defined as the equivalent number of wheels on a single vehicle which corresponds to the bending moment generated in a given main stringer by loading the structure with multiple vehicles. Distribution was found by taking stress readings across the width of the bridge on the tension flanges, at the centerline of the structure. The distribution was also checked by measuring deflections at the centerline with these deflection devices (Fig. 17), which gave deflections as electrical strain-gage readout.

Correlation between distribution factors found by stress and by deflection was very good. Since the bridge was erected in two halves, we were able to obtain wheel-load distribution factors for both a narrow and a wide bridge. The wheel-load distribution factor was found to vary with the width of structure, number of vehicles, and the type of vehicle. The maximum wheel-load distribution factor was found to occur with two of the short trucks positioned toward one side of the narrow bridge (Fig. 18).

This wheel-load distribution factor was found to be the equivalent of 97 percent of a single line of wheels, and occurred in the outside stringer. By comparison, this identical loading on the bridge twice as wide, produced a distribution factor of 68 percent for the same outside stringer. A factor of 100 percent had been used in the original design, corresponding to the AASHO factor S/4.0 for an open-grid steel deck. A wheel-load distribution factor of 1.0 was used in subsequent designs.

However, a single HS-20 vehicle traveling near the center lane of a wide bridge, generated a maximum distribution factor in any stringer of only 32 percent, indicating

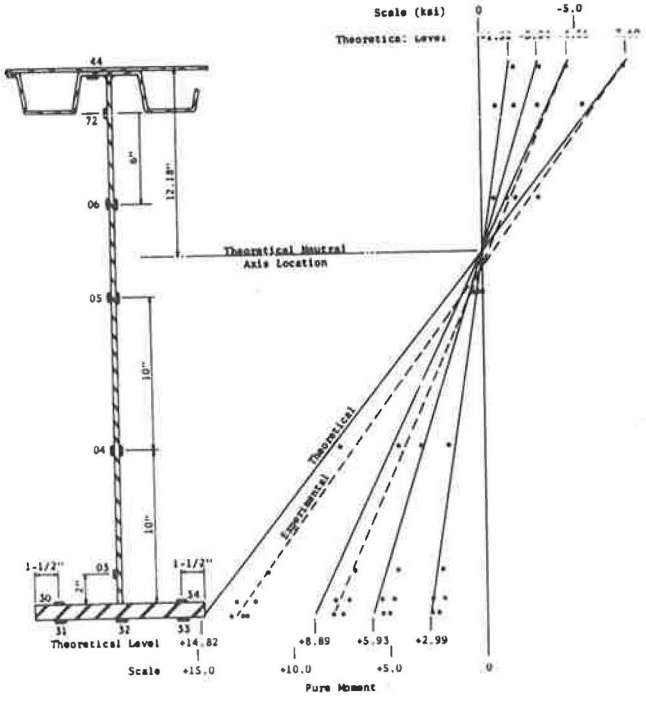

Figure 14. Comparison of neutral axis location—experimental vs theoretical.

Figure 15.

the significant reduction in stress afforded by the combination of greater bridge width and a single vehicle with better longitudinal distribution of wheel loads.

Local bending stresses in the deck assembly were found by placing the wheels of a small, specially-loaded flatbed truck (Fig. 19) between transverse floor beams. The

Figure 16.

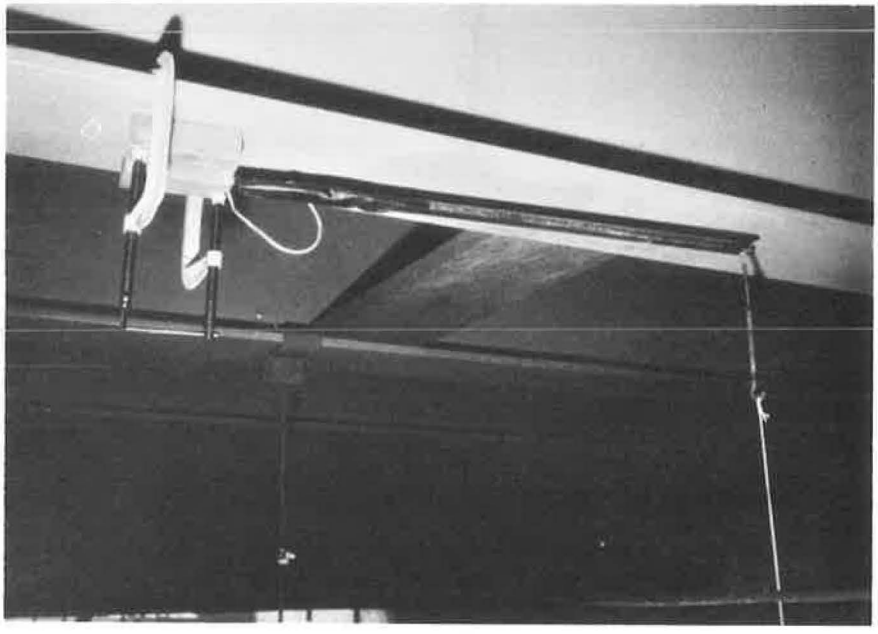

Figure 17.

dual tire on a single axle was weighted to 13,000 lb and the single tire was weighted to 10,700 lb (Fig. 20).

This weight on a single tire is unrealistically high, but provided a good comparative loading. The effect of the 13,000-lb wheel was prorated down to a 12,000-lb wheel, and the lighter wheel prorated upward to a 12,000-lb wheel to evaluate results on a comparative basis.

Figure 18.

Figure 19.

The critical local stress was found to occur at the bottom of a longitudinal rib, at the point where the rib passes over the floor beam. At this point the local stress is additive to the overall compressive bending stress.

Stresses were found to be sensitive to the number of tires, and to the load on the tires. Stresses were calculated in accordance with the procedures given in the AISC Orthotropic Design Manual.

It was found that the dual tire gave stresses about 14 percent less than those calculated. By comparison, the same weight on a single tire produced stresses about 8 percent greater than the AISC Design Manual value. The more meaningful result is associated with the loading on the dual tire, and indicates that reasonably close and conservative results can be expected using the AISC procedures.

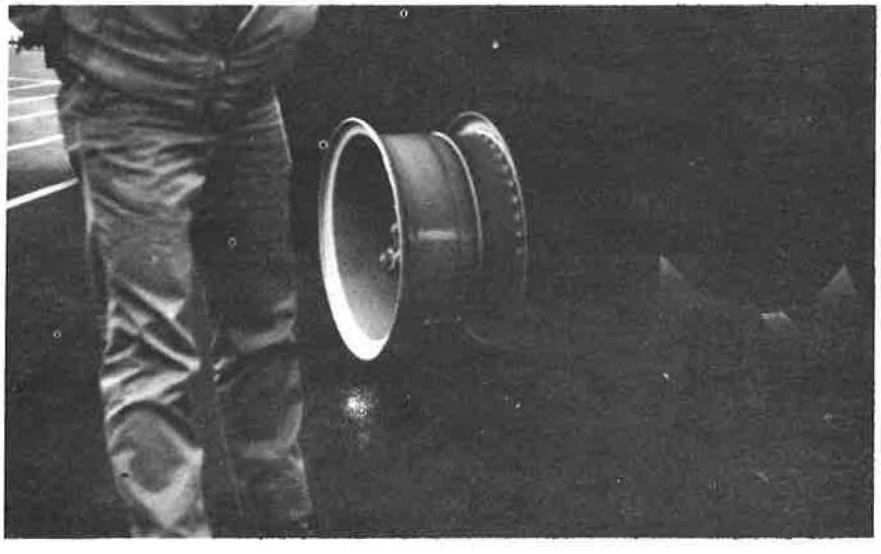

Figure 20.

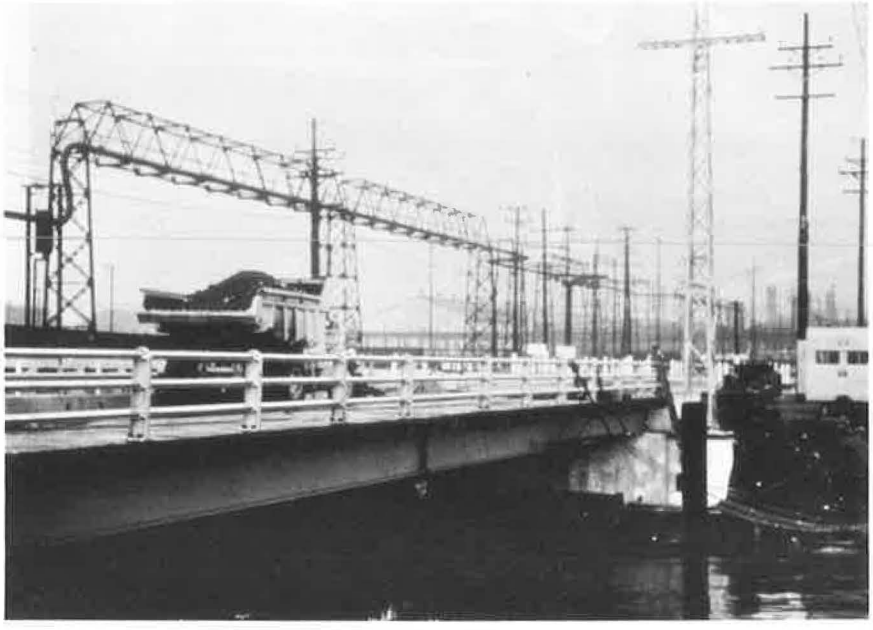

Figure 21.

Figure 22.

Figure 23.

Figure 24.

Another area of interest was the determination of dynamic loading effects on static stresses. The term "impact factor" is generally applied to this general increase in static loading effects. Impact factors were found using oscillographic readings for vehicles traveling at creep speed and again at speeds of 30 to 50 mph (Figures 21 through 23).

It was found that impacts did not exceed 10 percent for any of the trucks in overall bending. Impact factors for local stresses in the deck and transverse floor beams, under direct wheel loading from the trucks, went to about 30 percent. The 30 percent value is consistent with impacts obtained by using the AASHO Specifications, but the 10 percent values are less than half of those which would be prescribed by AASHO.

As to field performance (Fig. 24) of the roadway surfacing system over the past three years, we have found that the asphalt surfacing with epoxy membrane has provided a very satisfactory protection for the steel deck, and a smooth wearing surface. At this time, we have not detected any superiority of one type of asphalt over the other. The sliding Fabreeka-Teflon bearings have functioned well, with no sign of distress.

Results of the bridge tests, and observance of field performance, have been very enlightening and gratifying. Together they have adequately confirmed the behavior of the structure in accordance with theory, and have led to improvements in details and concepts for second-generation designs. One example of a detail improvement has been to adopt individual trapezoidal ribs in place of the continuous corrugation for easier fabrication and better weld inspection on future designs. Our knowledge of the structural behavior has led to greater confidence in the prediction of stresses, and in the establishment of dependable future design criteria for this type of structure.